Sparse Semi-Parametric Estimation of Harmonic Chirp Signals

J. SWÄRD, J. BRYNOLFSSON, A. JAKOBSSON AND
M. HANSSON-SANDSTEN

Published in: IEEE Transactions on Signal Processing
doi:10.1109/TSP.2015.2404314

Lund 2015

Mathematical Statistics
Centre for Mathematical Sciences
Lund University

Sparse Semi-Parametric Estimation of Harmonic Chirp Signals

Johan Swärd*, Johan Brynolfsson*, Andreas Jakobsson*, and Maria Hansson-Sandsten*

***Abstract*—In this work, we present a method for estimating the parameters detailing an unknown number of linear, possibly harmonically related, chirp signals, using an iterative sparse reconstruction framework. The proposed method is initiated by a re-weighted group-sparsity approach, followed by an iterative relaxation-based refining step, to allow for high resolution estimates. Numerical simulations illustrate the achievable performance, offering a notable improvement as compared to other recent approaches. The resulting estimates are found to be statistically efficient, achieving the corresponding Cramér-Rao lower bound.**

***Index Terms*—Harmonic chirps, multi-component, Block sparsity, LASSO, Cramér-Rao lower bound**

I. Introduction

MANY forms of everyday signals, ranging from radar and biomedical signals to seismic measurements and human speech, may be well modeled as signals with instantaneous frequencies (IF) that varies slowly over time [1]. Such signals are often modeled as linear chirps, i.e., periodic signals with an IF that changes linearly with time. Given the prevalence of such signals, much effort has gone into formulating efficient estimation algorithms of the start frequency and rate of development, and then, in particular, for signals only containing a single (complex-valued) chirp. One noteworthy such method is the phase unwrapping algorithm presented by Djuric and Kay [2]; further development of this method can be found in e.g. [3]. Other methods presented for single component estimation are, for example, based on Kalman filtering [4], [5], or sample covariance matrix estimates [6]. Similarly, in [7], the authors utilized the idea of single chirp modeling in detecting non-stationary phenomena in very noisy data. Recent work has to a larger extent focused on also identifying multi-component chirp signals, such as the maximum likelihood technique presented in [8], the fractional Fourier transform method [9]–[11], and the multitapered synchrosqueezed transform [12]. Others have used some Fourier based time-frequency estimate, e.g, the Wigner-Ville distribution, the reassigned spectrogram, or a Gabor dictionary, as a rough initial estimate, which may then be refined using image processing techniques to fit a linear chirp model [13]–[15]. The latter methods seem to render good estimates, although they typically require rather large data sets to do so. The reassignment method will yield perfect localization of the IF for each chirp component, given enough noise-free observations. Regrettably, it is quite sensitive to noise corruption [16]. Furthermore, in [17] a LASSO-based framework to estimate linear chirp signals was proposed that showed more robustness to noise as well as allowed for estimating an unknown number of unrelated linear chirps. Also, some efforts have been made to use a compressed sensing approach [18], where a dictionary containing a small number of chirps is formed and the final estimates are found using an FFT-based algorithm. The size of the dictionary was limited to the signal length, thus impairing the estimation abilities. Also, the method did not allow for any modeling of additional signal structure.

Often, the nonparametric methods have the advantage of computational efficiency, but generally also suffer from the poor resolution and high variance as is inherent to the spectrogram (see, e.g. [19]). The parametric methods on the other hand often have good performance and resolution, but generally require *a priori* knowledge of the number of components in the signal. Furthermore, it is not uncommon that one also needs to have good initial estimates to be able to use such methods; otherwise, the algorithm might suffer from convergence problems.

Many naturally occurring signals show a harmonic structure, i.e., a fundamental frequency with a number of overtones that are integer multiples of the fundamental frequency. For such signals there are many proposed algorithms (see e.g. [20]–[22]). However, in many signals the signal structure suffers from inharmonicities, such that the spectral components are not exactly harmonic. Recently, two works have also examined extensions to the case of a single source harmonic chirp, containing a set of harmonically related chirps signals [23], [24]. These signals have lately started to attract interest due to their ability to model non-stationary harmonical signals, such as many forms of audio signals [23]. In these works, both a nonlinear least squares (NLS) [23] and a maximum likelihood solution [24] were examined. In this work, we extend upon and generalize the findings in [17], to account for an harmonic structure, where both the number of sources and the number of harmonic overtones for each source are unknowns, as well as allow for the case when some of the harmonics are missing. The algorithm requires very few samples to get an accurate estimate of the parameters, which allows the method to also model short segments of even highly non-linear chirp signals

This work was supported in part by the Swedish Research Council, Knut and Alice Wallenberg's and Carl Trygger's foundations. This work has been presented in part at the Asilomar Conference on Signals, Systems, and Computers 2014.

*Dept. of Mathematical Statistics, Lund University, P.O. Box 118, SE-221 00 Lund, Sweden, emails: {js,johanb,aj,sandsten}@maths.lth.se.

as being piecewise linear over each of the segments, yielding a quite accurate *local* signal representation. Furthermore, as long as the sampling times are known, the algorithm will also handle irregularly sampled data. Typically, most existing works rely on available *a priori* knowledge of the order of the models, although such details are in general unavailable, and are notoriously hard to estimate [21]. Recently, some efforts on alleviating these assumptions have been made for purely harmonic signals [22], wherein a block-sparse framework is utilized to form the estimates. The here presented work extends on these efforts, also allowing for inharmonic sources, using the ideas introduced in [23]. We demonstrate the performance of the proposed method using both real and simulated data, and compare the results with the corresponding Cramér-Rao lower bound (CRLB), which is also presented, as well as with competing algorithms. To improve on the computational complexity, we present an efficient implementation, utilizing the alternating direction method of multipliers (ADMM) framework (see, e.g. [25]).

In this paper, scalars will be denoted with lower case symbols, e.g. x, whereas vectors will be denoted with bold lower case, $\mathbf{x}$. Matrices will be denoted with bold upper case letter, $\boldsymbol{X}$. Furthermore, $(\cdot)^T$, $(\cdot)^H$, $\Re$, and $\Im$ will be used to denote the transpose, the conjugate transpose, the real part, and the imaginary part, respectively.

The paper is structured as follows: In the next section, we introduce the signal model for harmonic chirp signals. Then, in section III, we derive the proposed algorithms and present some heuristics for setting the user parameters. In section IV, we present efficient implementations of the algorithms, whereas in section V, we illustrate the available performance of the introduced methods using numerical results. Finally, in section VI, we conclude upon our work.

II. Signal Model

Consider

$$y(t) = \sum_{k=1}^{K} \sum_{\ell=1}^{L_k} \alpha_{k,l} e^{i2\pi \ell \phi_k(t)} + e(t), \quad t = t_0, \ldots, t_{N-1} \tag{1}$$

where K and L_k denote the unknown number of fundamental chirps and the number of unknown harmonics for the kth component, respectively, whereas N denotes the number of available samples, t the sample times, which may be irregular, α_k the complex valued amplitude, $\phi_k(t)$ the time dependent frequency function, and $e(t)$ an additive noise term, here assumed to be white, circularly symmetric, and Gaussian distribution. Furthermore, the chirp signal is assumed to be reasonable linear, at least under short time intervals, which allows $\phi_k(t)$ to be modeled as

$$\phi_k(t) = f_k^0 t + \frac{r_k}{2} t^2 \tag{2}$$

yielding the IF function

$$\phi'_k(t) = f_k^0 + r_k t \tag{3}$$

where f_k^0 and r_k denote the starting frequency and the frequency rate, i.e., the frequency slope of the chirp, for chirp component k, respectively. The considered problem consists of estimating K, L_k, f_k^0, and r_k, as well as, in the process, also the phase, $\varphi_{k,\ell} \triangleq \angle \alpha_{k,\ell}$, and the magnitude, $a_{k,\ell} \triangleq |\alpha_{k,\ell}|$. Finally, we assume that $\min \{\ell \phi'_k(t)\} \geq 0$ and $\max \{\ell \phi'_k(t)\} \leq F_s$, $\forall (k,\ell)$, where F_s denotes the sampling frequency, in order to ensure that all frequencies in the signal are observable, i.e., fulfilling the Nyquist-Shannon sampling theorem.

III. Algorithm

In order to form an efficient algorithm for estimating the unknown parameters in (1), one may rewrite (1) as

$$\mathbf{y} = \tilde{\boldsymbol{D}} \tilde{\mathbf{a}} + \mathbf{e} \tag{4}$$

where

$$\mathbf{y} = \begin{bmatrix} y(t_0) & \ldots & y(t_{N-1}) \end{bmatrix}^T \tag{5}$$

$$\tilde{\mathbf{a}} = \begin{bmatrix} \alpha_{1,1} & \ldots & \alpha_{1,L_1} & \ldots & \alpha_{K,L_K} \end{bmatrix}^T \tag{6}$$

$$\tilde{\boldsymbol{D}} = \begin{bmatrix} \mathbf{d}_{1,1} & \ldots & \mathbf{d}_{1,L_1} & \ldots & \mathbf{d}_{K,L_K} \end{bmatrix} \tag{7}$$

$$\mathbf{d}_{k,\ell} = \begin{bmatrix} e^{i2\pi \ell \phi_k(t_0)} & \ldots & e^{i2\pi \ell \phi_k(t_{N-1})} \end{bmatrix}^T \tag{8}$$

and where $\mathbf{e}$ is formed in the same manner as $\mathbf{y}$. To allow for an unknown number of components, we expand the signal representation in (4) into one formed using a large dictionary containing $P \gg \sum_{k=1}^{K} L_k$ candidate chirps, such that

$$\mathbf{y} \approx \boldsymbol{D} \mathbf{a} \tag{9}$$

where $\boldsymbol{D}$ is an $N \times P$ dictionary matrix, and $\mathbf{a}$ the corresponding amplitudes, which thus mostly contains zeros, but with (at least) $\sum_{k=1}^{K} L_k$ non-zero elements. It is here assumed that P is selected sufficiently large so that the corresponding dictionary elements are close to the location of the true components and also spans the the relevant parameter space, e.g. ranging from 0 to F_s for the starting frequency parameter (see also [26], [27] for a related discussion). Solving (9) using ordinary least squares, if feasible, would yield a non-sparse solution, i.e., most of the indexes of $\mathbf{a}$ would be non-zero. Instead, we here impose the harmonic structure upon the solution by forcing it to choose between the different candidate chirp groups, while allowing for one or many of the overtones to be missing. To impose this structure, we form the minimization

$$\underset{\mathbf{x}}{\text{minimize}} \quad ||\mathbf{y} - \boldsymbol{D}\mathbf{x}||_2^2 + \lambda ||\mathbf{x}||_1 + \gamma \sum_{q=1}^{Q} ||\mathbf{x}[q]||_2 \tag{10}$$

where $\mathbf{x}[q]$ selects all elements in $\mathbf{x}$ corresponding to block q in $\boldsymbol{D}$, and Q denotes the number of blocks considered, where each block contains a fundamental chirp and its overtones, i.e., for block q, $\mathbf{x}[q]$ denotes the elements of $\mathbf{x}$ that corresponds to

$$\begin{bmatrix} \mathbf{d}_{q,1} & \ldots & \mathbf{d}_{q,L_q} \end{bmatrix} \tag{11}$$

in the dictionary. The first term in (10) measures the distance between the signal and the model, the second term enforces an overall sparsity between the available chirp candidates and thus limits the number of chirps that may be part of the solution. The third term in (10) acts as a sparsity enhancer for the number of harmonically related chirp groups that are allowed in the solution, thus promoting a solution that has fewer number of activated groups. Together, the two last terms in (10) promotes a solution that has few harmonically related chirp groups, and also allows for chirps within a group to be sparse.This optimization problem is convex as it is a sum of convex functions, and the solution may thus be found using standard interior-point methods, such as, e.g., SeDumi [28] and SDPT3 [29]. Furthermore, γ and λ are tuning parameters controlling the sparsity of the groups and the sparsity within the groups, respectively. It is worth noting that if setting $\gamma = 0$, one solves the problem of finding unrelated chirps in the signal. Even though P is finely spaced, the quality of the solution obtained from (10) will depend on the grid structure of $\boldsymbol{D}$, i.e., if the true components are not contained in the dictionary, the components that are the closest to the true chirps will be activated, ensuring that the corresponding indices in $\mathbf{x}$ will be non-zero. Therefore, the solution attained from (10) will be biased in accordance to the chosen grid structure of $\boldsymbol{D}$. To avoid this bias, the estimation procedure involves an additional step consisting of a nonlinear least squares (NLS) search to further increase the resolution. In order to do so, let the residual from (10) be formed as

$$\mathbf{r} = \mathbf{y} - \boldsymbol{D}\mathbf{x} \tag{12}$$

Then, each harmonic chirp component may be iteratively updated by first adding one component to the residual formed in (12), conducting a NLS search for the parameter estimates, initiated using the estimates found from (10), and then remove the found component using (12). When all components have been updated in this way, one may continue updating the residual with the newly refined estimates. The final estimates are found by iterating the entire refinement procedure a few times.

In the above algorithm, the user has to select a value for the parameters γ and λ. Of these, the value of γ penalizes the number of harmonic chirps allowed in the solution, meanwhile the value of λ penalizes the overall number of chirps, thus allowing for sparsity within each harmonic chirp component. The values of γ and λ are commonly chosen through cross-validation [30], or by some data dependent heuristics. In the case of $\gamma = 0$, we herein suggest selecting

$$\lambda = \frac{||\mathbf{y}||_2^2}{2N} \tag{13}$$

which has empirically been shown to provide a reliable choice of λ, for the here considered data lengths. When both tuning parameters are active, the problem of setting good values becomes more complicated, since the two penalties interact. We have empirically found that, as long as λ is reasonably small, one may use (13) as a rule of thumb for also setting γ. To further increase the robustness to the choice of γ and λ, and to further enhance the sparsity, we propose a re-weighted approach, based on the technique introduced in [31]. In this approach, one solves the minimization iteratively, where, at every iteration, two weight matrices, $\boldsymbol{W}$ and $\mathbf{V}$, with weights $w_1, \ldots, w_P$ and $v_1, \ldots, v_Q$ on the diagonals and zeros elsewhere, are used. The diagonal elements in $\boldsymbol{W}$ and $\mathbf{V}$ are

Algorithm 1 The HSMUCHES algorithm

Initiate $w_p = 1$, for $p = 1, \ldots, P$, and $v_q = 1$, for $q = 1, \ldots, Q$
for $b = 1, \ldots$ **do**
    Solve (16)
    Update (14) and (15)
end for
Compute (12)
for j = 1,... **do**
    for $k = 1, \ldots, \hat{K}$ **do**
        $\mathbf{z} = \mathbf{r} + \boldsymbol{D}(\cdot, \boldsymbol{I}_{\hat{K}}(k))^{(j)}\mathbf{x}(\boldsymbol{I}_{\hat{K}}(k))^{(j)}$
        Using $\mathbf{z}$, update $\boldsymbol{D}(\cdot, \boldsymbol{I}_{\hat{K}}(k))^{(j)}$ and $\mathbf{x}(\boldsymbol{I}_{\hat{K}}(k))^{(j)}$ via NLS
        Subtract the refined estimates from $\mathbf{z}$
    end for
end for

updated as

$$w_p^{(b)} = \frac{1}{|x_p^{(b-1)}| + \epsilon}, \qquad p = 1, \ldots, P \tag{14}$$

$$v_q^{(b)} = \left(\frac{1}{||\mathbf{x}^{(b-1)}[q]||_2^2 + \epsilon} \right)^{1/2}, \qquad q = 1, \ldots, Q \tag{15}$$

where the superscript b denotes the iteration number, and $\epsilon > 0$ is a small offset parameter, which prevents the solution from diverging. At each iteration, one thus solves

$$\underset{\mathbf{x}}{\text{minimize}} \quad ||\mathbf{y} - \boldsymbol{D}\mathbf{x}||_2^2 + \lambda ||\boldsymbol{W}^{(b)}\mathbf{x}||_1 + \gamma \sum_{q=1}^{Q} v_q^{(b)} ||\mathbf{x}[q]||_2 \tag{16}$$

The resulting algorithm is outlined in Algorithm 1, where $\boldsymbol{D}(\cdot, k)$ and $\mathbf{x}(k)$ denote the kth column and the kth index of the matrix $\boldsymbol{D}$ and the vector $\mathbf{x}$, respectively. Furthermore, let $\hat{K}$ denote the number of non-zero elements in the solution from (10), and let the corresponding indices in $\mathbf{x}$ make up the index set $\boldsymbol{I}_{\hat{K}}$. Clearly, one must select an appropriate stopping criteria for the second loop in Algorithm 1. This may be done in various ways, such as when the parameter estimates does no longer improve significantly in each iteration, or by setting a maximum number of iterations. Empirically, we found that 10 iterations where enough for convergence and through out this work, we used this as stopping criteria. It should be noted that the re-weighted approach introduces the tuning parameter ϵ. In this paper, we have set ϵ to be

$$\epsilon = \frac{N}{||\mathbf{y}||_2^2} \tag{17}$$

which is in accordance with the discussion in [31], and which has been empirically shown to yield reliable estimates.

It should be noted that if $\gamma = 0$, the estimator does not assume any harmonic structure, and therefore constitutes solely a multi-chirp estimator; we term this the Sparse MUlti-component Chirp EStimator (SMUCHES). In the case $\gamma > 0$, the estimator also allows for the possibility of harmonic chirp components; we term this the Harmonic Sparse MUlticomponent Chirp EStimator (HSMUCHES).

IV. Efficient Implementation

We proceed to examine efficient implementations of the proposed estimators using the ADMM framework. The discussion here is focused on the HSMUCHES estimator, although the implementation also works for the SMUCHES algorithm by simply setting $\gamma = 0$. In general, an ADMM solves problems in the form

$$\begin{aligned} \underset{\mathbf{x},\mathbf{z}}{\text{minimize}} \quad & f(\mathbf{x}) + g(\mathbf{z}) \\ \text{subject to} \quad & \mathbf{A}\mathbf{x} + \mathbf{B}\mathbf{z} = c \end{aligned} \tag{18}$$

In our case, $\mathbf{A} = \boldsymbol{I}$, $\mathbf{B} = -\boldsymbol{I}$, $c = 0$, $f(\mathbf{x}) = ||\mathbf{y} - \boldsymbol{D}\mathbf{x}||_2^2$, and $g(\mathbf{z}) = \lambda||\mathbf{z}||_1 + \gamma\sum_{q=1}^{Q}||\mathbf{z}[q]||_2$, where $\boldsymbol{I}$ denotes the identity matrix of size $N \times P$. The augmented Lagrangian for this minimization is formed as

$$L_\rho(\mathbf{x},\mathbf{z},\mathbf{u}) = f(\mathbf{x}) + g(\mathbf{z}) + \frac{\rho}{2}||\mathbf{x} - \mathbf{z} + \mathbf{u}||_2^2 \tag{19}$$

where $\mathbf{u}$ is the scaled dual variable, and ρ is the penalty parameter, penalizing the distance between $\mathbf{z}$ and $\mathbf{x}$. The ADMM finds the solution to (16) by iteratively solving (19) for each variable separately. The steps in the ADMM are

$$\mathbf{x}^{(k+1)} = \underset{\mathbf{x}}{\text{argmin}}\left(f(\mathbf{x}) + \frac{\rho}{2}||\mathbf{x} - \mathbf{z}^{(k)} + \mathbf{u}^{(k)}||_2^2\right) \tag{20}$$

$$\mathbf{z}^{(k+1)} = \underset{\mathbf{z}}{\text{argmin}}\left(g(\mathbf{z}) + \frac{\rho}{2}||\mathbf{x}^{(k+1)} - \mathbf{z} + \mathbf{u}^{(k)}||_2^2\right) \tag{21}$$

$$\mathbf{u}^{(k+1)} = \mathbf{x}^{(k+1)} - \mathbf{z}^{(k+1)} + \mathbf{u}^{(k)} \tag{22}$$

To find the solution to (20), one differentiates (19) with respect to $\mathbf{x}$ and put it equal to zero, yielding

$$\mathbf{x}^{(k+1)} = \left(\boldsymbol{D}^H\boldsymbol{D} + \rho\boldsymbol{I}\right)^{-1}\left(\boldsymbol{D}^H\mathbf{y} + \rho\left(\mathbf{z}^{(k)} - \mathbf{u}^{(k)}\right)\right) \tag{23}$$

To solve (21), one needs to take some further care as $g(\mathbf{z})$ is not differentiable at $\mathbf{z} = 0$. However, it can be shown (see e.g. [32]) that the solution to (21) is

$$\mathbf{z}^{(k+1)} = \boldsymbol{\mathcal{S}}\left(\mathbf{S}\left(\mathbf{x}^{(k+1)} + \mathbf{u}^{(k)}, \lambda/\rho\right), \gamma/\rho\right) \tag{24}$$

where $\mathbf{S}$ and $\boldsymbol{\mathcal{S}}$ are soft thresholds defined as

$$\mathbf{S}(\mathbf{x},\kappa) = \frac{x_j}{|x_j|}\max(|x_j| - \kappa, 0) \tag{25}$$

$$\boldsymbol{\mathcal{S}}(\mathbf{x},\kappa) = \frac{\mathbf{x}[q]}{||\mathbf{x}[q]||_2}\max(||\mathbf{x}[q]||_2 - \kappa, 0) \tag{26}$$

for $q = 1, \ldots, Q$, where $\mathbf{S}$ should be interpreted element-wise. Observing that $f(\mathbf{x})$ and $g(\mathbf{z})$ are closed, proper, and convex functions, and given $\rho > 0$, then, under some mild assumptions, if there is a solution to (16), then the algorithm will converge to this solution [33], [34]. Also, the choice of ρ will only effect the convergence rate, not whether or not the method will converge. Using this implementation, the computational complexity for SMUCHES is, for the Lasso part, $\mathcal{O}(N^3 + N^2P)$. The computations in this part are dominated by (23), which only needs to be calculated once throughout the minimization. Furthermore, the computational complexity of the inverse is significantly decreased using the Woodbury matrix identity [35]. The NLS part of the proposed algorithm requires a computational complexity of $\mathcal{O}(\hat{K}NP)$.

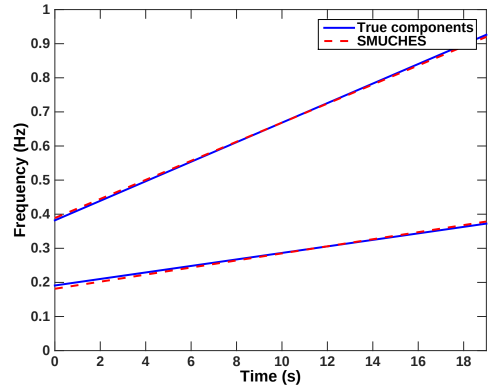

Fig. 1. The figure shows the true (solid) and the estimated (dashed) IF.

It may be noted that a dictionary similar to (7) was proposed in [18]; in this case, the dictionary was restricted to only contain N candidate chirps. As a result, the dictionary experienced low correlation between the columns, for which case the restricted isometry properties (RIP) will hold, suggesting that the signal may be recovered with high probability (see, e.g., [36]). The same result would hold for the dictionary in (7), if restricted in the same manner. However, to allow for high resolution estimates, the dictionary should, as discussed, be extended to contain many more chirp candidates, indicating that the dictionary columns will be highly correlated, thereby no longer satisfying the RIP. Fortunately, as is also shown in the next section, practical evidence indicate that even highly correlated dictionaries enjoy excellent signal recovery properties.

V. Numerical Results

In order to evaluate the performance of the proposed algorithms, we examine their behavior on both real and simulated data, comparing them both to other alternative techniques, and to the CRLB (as derived in Appendix A). All the following root mean squared error (RMSE) curves are based on 1000 Monte Carlo simulations.

Initially, we examine a simulated uniformly sampled signal of length $N = 20$, consisting of two non-harmonic chirp components, as depicted in Figure 1, which is corrupted by white circularly symmetric Gaussian noise with a signal to noise ratio (SNR) of 10 dB, which is here defined as

$$\text{SNR} = 10\log_{10}\left(\frac{P_{\mathbf{y}}}{\sigma^2}\right) \tag{27}$$

where $P_{\mathbf{y}}$ denotes the power of the signal, and σ^2 the variance of the additive noise. The resulting estimates from the proposed SMUCHES method and for the reassigned spectrogram [16] are shown in Figures 1 and 2, respectively. As can be seen in Figure 2, the reassigned spectrogram finds the two chirp components, but the estimates are blurred, as well exhibiting jumps in the frequencies. On the other hand, as can be seen

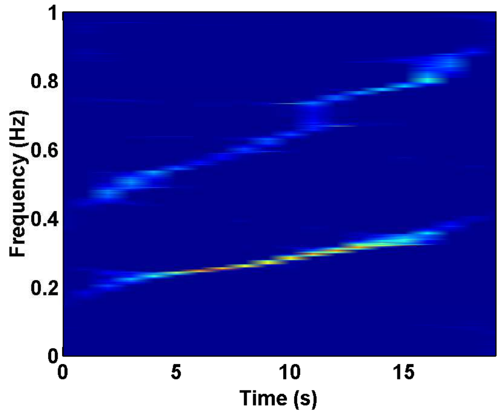

Fig. 2. The figure shows the estimated time-frequency distribution of the chirp signals using the reassigned spectrogram.

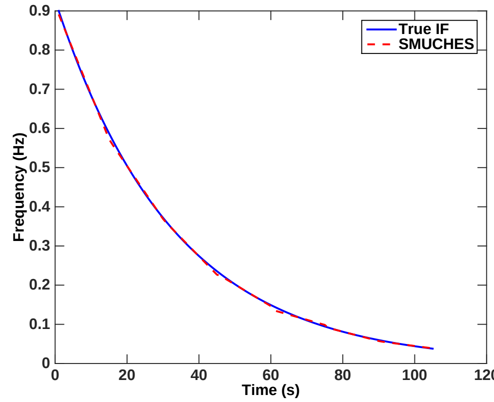

Fig. 3. The estimated chirp in dashed lines as compared to the true chirp.

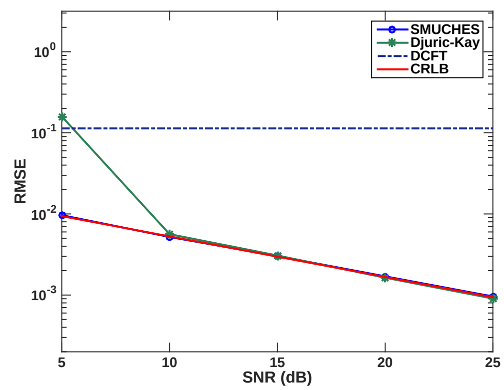

Fig. 4. Performance of the proposed SMUCHES method, as compared with the Djuric-Kay method, the DCFT method, and the CRLB, when estimating the starting frequency of a single chirp.

in Figure 1, the proposed method manages to find the chirp components without any such ambiguities.

We continue by showing how the proposed SMUCHES method may be used in tracking a non-linear chirp. In this example, we simulated an exponential chirp component defined as

$$\phi(t) = \left(\frac{r^t - 1}{\log(r)}\right) f_0 \tag{28}$$

where f_0 and r are parameters determining the starting frequency and the exponential rate of change, respectively. The signal, containing $N = 105$ samples, was divided in 7 equally sized sections, such that each segment may be reasonably well modeled as a linear chirp. The signal was corrupted by a white circularly symmetric Gaussian noise with SNR $= 20$ dB. The proposed algorithm was applied on each signal segment. The resulting chirp estimate is depicted in Figure 3, where it is clearly shown how the proposed method manages to estimate the evolving parameters of the non-linear chirp, showing that the local linear approximation is valid.

Next, we examine the estimation performance of the SMUCHES method as a function of SNR. In this example, the simulated signal contains only a single chirp component, with starting frequency $f^0 = 0.6/\pi$, frequency rate $r = 0.03/\pi$, amplitude $\alpha = 1$, and a uniformly distributed random phase $\varphi \in U[-\frac{1}{2}, \frac{1}{2})$, which was randomized for each simulation. The sample length is set to $N = 20$.

Figures 4 and 5 show the RMSE of the SMUCHES estimator, where λ and ϵ were selected using (13) and (17), as well as the discrete chirp Fourier transform algorithm (DCFT) [9], the algorithm presented by Djuric and Kay in [2], both being allowed oracle knowledge of the number of chirps in the signal, and the CRLB. It should be noted that the proposed methods do not assume any model order information, as they are estimating this as part of the optimization; clearly, this also implies that the method may estimate the wrong model orders. However, the proposed SMUCHES method only estimated the wrong number of components in 1 out of the 1000 simulations, and this at the SNR $= 5$ dB level. For the other SNR levels, the order estimations were without any errors. To assert a fair comparison, the simulation where the proposed method estimated the wrong model order was removed from all methods, and is thus not included in the RMSE graphs. As is clear from Figures 4 and 5, the SMUCHES method, without using any prior knowledge about the number of chirps, manages to attain the CRLB, as well as outperforming the Djuric-Kay algorithm, even though the latter has been allowed oracle model order information. Furthermore, it can be seen that the DCFT algorithm is stuck to its initial grid, which suggests why it does not manage to improve beyond a certain limit when the SNR increases. Examining the computational complexities, it was found that the Djuric-Kay and the DCFT algorithms (given oracle model orders) are notably faster to compute than the presented SMUCHES implementation, requiring on average (computed over 1000 simulations on a regular PC, for SNR$=$ 20 dB) $2.3 \cdot 10^{-4}$, $5.1 \cdot 10^{-3}$, and $5.0 \cdot 10^{-1}$ seconds to execute, respectively.

We proceed by examining the performance on multicomponent chirp signals. Since the competing methods, which we previously compared with, cannot be used on multicomponent data, we only show the results for the proposed method as compared to the corresponding CRLB. Figure 6 depicts the RMSE of the parameter estimations, as a function of SNR.

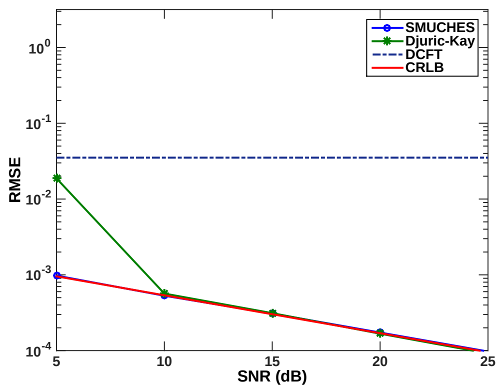

Fig. 5. Performance of the proposed SMUCHES method, as compared with the the Djuric-Kay method, the DCFT method, and the CRLB, when estimating the frequency rate of a single chirp.

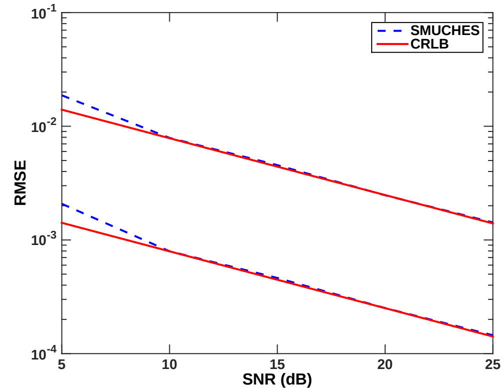

Fig. 6. Performance of the proposed SMUCHES method when estimating the starting frequencies (top curves) and the frequency rates (bottom curves) of two non-crossing linear chirps, as compared to the CRLB.

The starting frequency of the chirps were $f_1^0 = 0.6/\pi$ and $f_2^0 = 1.2/\pi$, and the slope rates were $r_1 = 0.03/\pi$ and $r_2 = 0.09/\pi$. The amplitudes were set to unity and the phase were drawn as $\varphi \in U[-\frac{1}{2}, \frac{1}{2})$ at each simulation. Once again, λ and ϵ were chosen using (13) and (17). As one can note from Figure 6, the proposed method follows the CRLB for SNR levels greater or equal to 10 dB. In this case, the proposed method estimated the wrong model order 26 times out of the 1000 simulations, all for the SNR = 5 dB case, and not at all for higher SNRs. Again, these simulations were removed from the proposed method's RMSE, and the CRLB was adjusted correspondingly. Next, we examine the performance on irregularly sampled data constituting of 20 observations from a chirp signal with the same chirp components as in the previous example. The sampling times where drawn from a rectangular distribution in the range $(0, 20]$ and are depicted in Figure 7. The phase was drawn from $U[-\frac{1}{2}, \frac{1}{2})$ for each simulation. Figure 8 shows the resulting RMSE results. As for the earlier examples, for SNR greater than 5 dB, the proposed method attains the CRLB. The main difference to the uniform sampled case is that the resulting RMSE for SNR = 5 dB is worse. Also, the number of times the proposed method estimated the wrong model order increased to 51 times out of 1000, again, only for the SNR = 5 dB case. As before, for SNR greater than 5 dB, no errors in the model order estimation were made. Though slightly more sensitive to non-uniformly sampled data, it can be concluded that the proposed method is suitable to use also for non-uniformed sampled data.

We proceed to examine the performance on simulated harmonic data. The simulated chirp signal consist of one fundamental frequency and 3 overtones ($K = 1$ and $L_1 = 4$), each with unit amplitude and uniformly distributed random phase. The fundamental starting frequency was set to $f^0 = 0.2 * 3/\pi$ and the frequency slope to $r = -0.004 * 3/\pi$. The resulting RMSE are shown in Figures 9 and 10, as a function of SNR, when using $N = 20$ samples. The RMSEs for both the starting frequency and the frequency slope, are measured as mean value of the RMSE for each of the four components in the signal, i.e., for the fundamental frequency and the two

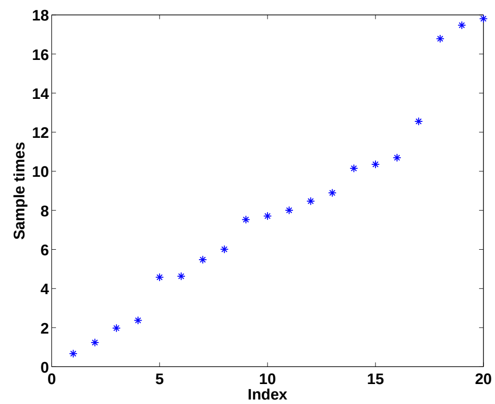

Fig. 7. The distribution of the sample times.

overtones. Here, HSMUCHES estimated the wrong model order 54 times out of 1000 at SNR = 5 dB, 5 times out of 1000 at SNR = 10 dB, and made no mistakes at higher SNRs.

As SMUCHES does not take the harmonicity inherent in the signal in account, there are 18 parameters (model order, noise variance, and four parameters for each component) to estimate using only 20 samples, whereas HSMUCHES only has to estimate twelve parameters (model order, number of overtones, starting frequency, frequency slope, phase, noise variance, and four amplitudes). As a result, it can be expected that SMUCHES will make more order estimation mistakes than HSMUCHES, which was also found to be the case. Out of the 1000 simulations, SMUCHES made 906 model order errors at SNR=5 dB, 261 at SNR=10 dB, 21 at SNR=15 dB, 8 at SNR = 20 dB, and 3 errors at SNR = 25 dB. The tuning parameters for SMUCHES were selected using (13) and (17), and for HSMUCHES γ using (13), with $\lambda = 0$, and $\epsilon = 10^{-4}$. Finally, we show the performance on real data, containing sounds from bats [37]. Many forms of audio sources, such as voiced speech and many forms of music, may be well modelled as harmonic signals. Thus, it should be expected that the sound from a bat may contain a harmonic structure.

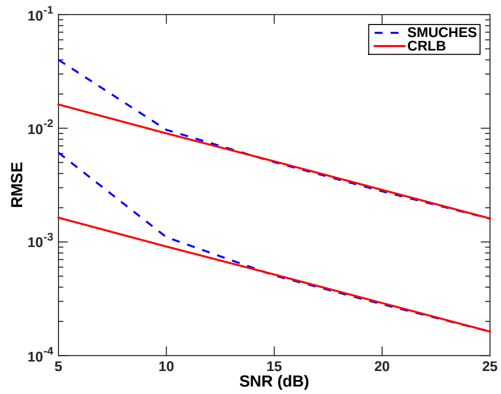

Fig. 8. Performance of the proposed SMUCHES method when estimating the starting frequencies (top curves) frequency rates (bottom curves) of two non-crossing linear chirps for irregularly sampled data, as compared to the CRLB.

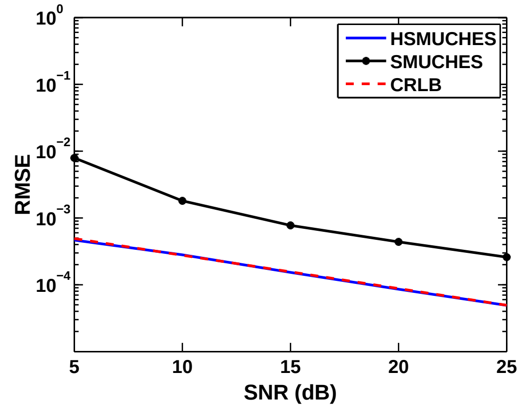

Fig. 10. Performance of the proposed HSMUCHES methods applied to an harmonic chirp signal with one fundamental frequency and three overtones, as compared with the SMUCHES method and the CRLB, when estimating the frequency slopes.

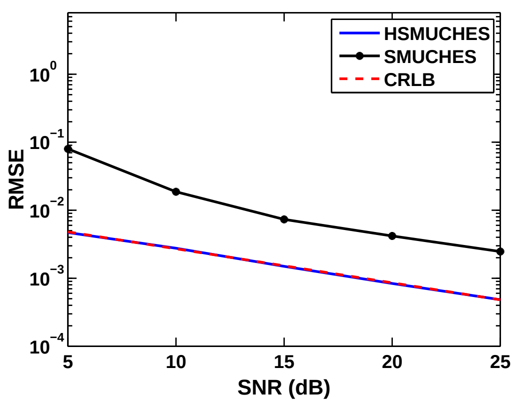

Fig. 9. Performance of the proposed HSMUCHES methods applied to an harmonic chirp signal with one fundamental frequency and three overtones, as compared with the SMUCHES method and the CRLB, when estimating the starting frequencies.

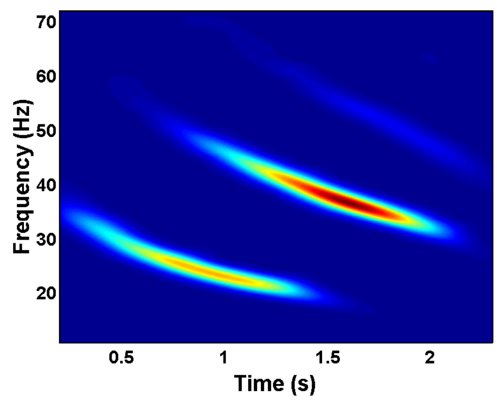

Fig. 11. The figure shows the spectrogram of the bat chirp.

The spectrogram of the bat signal is shown in Figure 11, suggesting that the signal contains one fundamental chirp with, at most, two overtones. Figure 12 shows the estimated harmonic structure when using HSMUCHES. Comparing the figures, it is clear that the HSMUCHES algorithm is well able to capture the changing frequencies in the harmonic signal, achieving a substantially better resolution than the spectrogram. As before, the tuning parameters for SMUCHES were selected using (13) and (17), and for HSMUCHES, γ was set to two times (13), $\lambda = 0.01$, and $\epsilon = 10^{-4}$.

VI. Conclusion

In this paper, we have proposed two semi-parametric algorithms for estimating the parameters of an unknown number of chirp and harmonic chirp components in noisy data, respectively. The methods are shown to work well even for very short signals, and allow for both uniform and non-uniform sampled data. The methods are shown to attain the corresponding CRLB for both cases. Furthermore, it is shown in the paper that the methods can be also used to approximate non-linear chirps, by dividing the data into small sections, in which the non-linear chirps can be assumed to be reasonably linear. Numerical examples illustrate the preferable performance on both real and simulated signals.

VII. Acknowledgement

The author wishes to thank Curtis Condon, Ken White, and Al Feng of the Beckman Institute of the University of Illinois for the bat data and for permission to use it in this paper.

Appendix A
Cramér-Rao Lower Bound

The CRLB for a multi-component chirp signal has been derived in multiple papers, see e.g. [8]. Here, we derive the CRLB for the case of both regular frequencies and irregular sampling, as well as harmonic overtones. The Fisher information matrix (FIM) for any signal observed under complex valued additive white noise, with variance σ^2, can be set up block-wise as

$$J_{ij} = \frac{2}{\sigma^2} \sum_{n=0}^{N-1} \left(\frac{\partial \Re\{y(t_n)\}}{\partial \theta_i} \frac{\partial \Re\{y(t_n)\}}{\partial \theta_j} + \frac{\partial \Im\{y(t_n)\}}{\partial \theta_i} \frac{\partial \Im\{y(t_n)\}}{\partial \theta_j} \right) \tag{29}$$

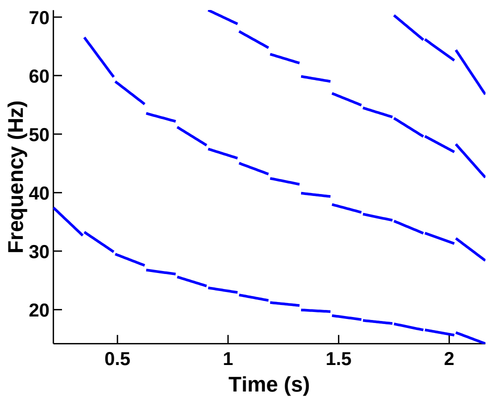

Fig. 12. The figure shows the estimated time-frequency content of the bat signal using the proposed HSMUCHES algorithm.

where $\theta_k = [f_k^0 \,,\, r_k \,,\, \varphi_{k,1} \,,\, \ldots \,,\, \varphi_{k,L_k} \,,\, \alpha_{k,1} \,,\, \ldots \,,\, \alpha_{k,L_k}]^T$, L_k is the number of harmonics, and $\alpha_{k,\ell}$ is the kth amplitude of the ℓth harmonic. Hence, the FIM will have $(K \times K)$ blocks, such that

$$\boldsymbol{J} = \begin{bmatrix} \boldsymbol{J}_{11} & \boldsymbol{J}_{12} & \cdots & \boldsymbol{J}_{1K} \\ \boldsymbol{J}_{21} & \boldsymbol{J}_{22} & \cdots & \boldsymbol{J}_{2K} \\ \cdots & \cdots & \ddots & \vdots \\ \boldsymbol{J}_{K1} & \boldsymbol{J}_{K2} & \cdots & \boldsymbol{J}_{KK} \end{bmatrix} \tag{30}$$

By denoting the Fisher information between the two parameters u and v as

$$\mathcal{I}(u,v) \triangleq \frac{\partial \Re\{y(t_n)\}}{\partial u}\frac{\partial \Re\{y(t_n)\}}{\partial v} + \frac{\partial \Im\{y(t_n)\}}{\partial u}\frac{\partial \Im\{y(t_n)\}}{\partial v} \tag{31}$$

each block in the FIM may be found as

$$\boldsymbol{J}_{kj} = \frac{2}{\sigma^2}\sum_{n=0}^{N-1}\begin{bmatrix} \mathcal{I}\left(\theta_k(1), \theta_j(1)\right) & \cdots & \mathcal{I}\left(\theta_k(1), \theta_j(M_j)\right) \\ \vdots & \ddots & \vdots \\ \mathcal{I}\left(\theta_k(M_k), \theta_j(1)\right) & \cdots & \mathcal{I}\left(\theta_k(M_k), \theta_j(M_j)\right) \end{bmatrix}$$

where $M_k = 2 + 2L_k$ denotes the number of parameters for the kth component. Defining

$$\Psi_{k,\ell}(t_n) \triangleq 2\pi\left(\ell\left(f_k^0 t_n + \frac{r_k}{t_n}t_n^2\right) + \varphi_k\right) \tag{32}$$

and

$$\Delta\Psi_{k,\ell,j,m}(t_n) \triangleq \Psi_{k,\ell}(t_n) - \Psi_{j,m}(t_n) \tag{33}$$

each pairwise Fisher information is found as

$$\begin{aligned}
\mathcal{I}(f_k, f_j^0) &= \sum_{\ell=1}^{L_k}\sum_{m=1}^{L_j} \alpha_{k,\ell}\alpha_{j,m}4\pi^2\ell m t_n^2 \cos\Delta\Psi_{k,\ell,j,m}(t_n) \\
\mathcal{I}(f_k^0, r_j) &= \sum_{\ell=1}^{L_k}\sum_{m=1}^{L_j} \alpha_{k,\ell}\alpha_{j,m}2\pi^2\ell m t_n^3 \cos\Delta\Psi_{k,\ell,j,m}(t_n) \\
\mathcal{I}(f_k^0, \varphi_{j,m}) &= \sum_{\ell=1}^{L_k} \alpha_{k,\ell}\alpha_{j,m}4\pi^2\ell t_n \cos\Delta\Psi_{k,\ell,j,m}(t_n) \\
\mathcal{I}(f_k^0, \alpha_{j,m}) &= \sum_{\ell=1}^{L_k} -\alpha_k 2\pi\ell t_n \sin\Delta\Psi_{k,\ell,j,m}(t_n) \\
\mathcal{I}(r_k, f_j^0) &= \sum_{\ell=1}^{L_k}\sum_{m=1}^{L_j} \alpha_{k,\ell}\alpha_{j,m}2\pi^2\ell m t_n^3 \cos\Delta\Psi_{k,\ell,j,m}(t_n) \\
\mathcal{I}(r_k, r_j) &= \sum_{\ell=1}^{L_k}\sum_{m=1}^{L_j} \alpha_{k,\ell}\alpha_{j,m}\pi^2\ell m t_n^4 \cos\Delta\Psi_{k,\ell,j,m}(t_n) \\
\mathcal{I}(r_k, \varphi_{j,m}) &= \sum_{\ell=1}^{L_k} \alpha_{k,\ell}\alpha_{j,m}2\pi^2\ell t_n^2 \cos\Delta\Psi_{k,\ell,j,m}(t_n) \\
\mathcal{I}(r_k, \alpha_{j,m}) &= \sum_{\ell=1}^{L_k} -\alpha_{k,l}\pi\ell t_n^2 \sin\Delta\Psi_{k,\ell,j,m}(t_n) \\
\mathcal{I}(\varphi_k, f_j^0) &= \sum_{\ell=1}^{L_k}\sum_{m=1}^{L_j} \alpha_{k,\ell}\alpha_{j,m}4\pi^2 m t_n \cos\Delta\Psi_{k,\ell,j,m}(t_n) \\
\mathcal{I}(\varphi_k, r_j) &= \sum_{\ell=1}^{L_k}\sum_{m=1}^{L_j} \alpha_{k,\ell}\alpha_{j,m}2\pi^2 m t_n^2 \cos\Delta\Psi_{k,j,\ell,m}(t_n) \\
\mathcal{I}(\varphi_{k,\ell}, \varphi_{j,m}) &= \alpha_{k,\ell}\alpha_{j,m}4\pi^2 \cos\Delta\Psi_{k,\ell,j,m}(t_n) \\
\mathcal{I}(\varphi_k, \alpha_{j,m}) &= \sum_{\ell=1}^{L_k} -\alpha_{k,\ell}2\pi \sin\Delta\Psi_{k,\ell,j,m}(t_n) \\
\mathcal{I}(\alpha_{k,\ell}, f_j^0) &= \sum_{m=1}^{L_j} \alpha_{j,m}2\pi m t \sin\Delta\Psi_{k,\ell,j,m}(t_n) \\
\mathcal{I}(\alpha_{k,\ell}, r_j) &= \sum_{m=1}^{L_j} \alpha_{j,m}\pi m t_n^2 \sin\Delta\Psi_{k,\ell,j,m}(t_n) \\
\mathcal{I}(\alpha_{k,\ell}, \varphi_{j,m}) &= \alpha_{j,m}2\pi \sin\Delta\Psi_{k,\ell,j,m}(t_n) \\
\mathcal{I}(\alpha_{k,\ell}, \alpha_{j,m}) &= \cos\Delta\Psi_{k,\ell,j,m}
\end{aligned}$$

Finally, the CRLB is found as the inverse of the FIM.

REFERENCES

[1] P. Flandrin, "Time-Frequency and Chirps," in *Wavelet Applications VIII*, 2001.

[2] P. Djurić and S. Kay, "Parameter Estimation of Chirp Signals," *IEEE Transactions on Acoustics Speech and Signal Processing*, vol. 38, pp. 2118–2126, 1990.

[3] O. Besson, M. Ghogho, and A. Swami, "Parameter Estimation for Random Amplitude Chirp Signals," *IEEE Transactions on Signal Processing*, vol. 47, no. 12, pp. 3208–3219, 1999.

[4] I. Rusnak and L. Peled-Eitan, "New Approach to Estimation of Chirp Signal with Unknown Parameters," in *IEEE International Conference on Microwaves, Communications, Antennas and Electronics Systems*, Tel Aviv, Israel, Oct. 21-23 2013.

[5] J. Gal, A. Campeanu, and I. Nafornita, "The Estimation of Chirp Signals Parameters by an Extended Kalman Filtering Algorithm," in *10th International Symposium on Signals, Circuits and Systems*, Iasi, Romania, June 30- July 1 2011.

[6] B. Völcker and B. Ottersten, "Chirp Parameter Estimation from a Sample Covariance Matrix," *IEEE Transactions on Signal Processing*, vol. 49, no. 3, pp. 603–612, March 2001.

[7] E. Candes, P. Charlton, and H. Helgason, "Detecting Highly Oscillatory Signals by Chirplet Path Pursuit," 2006, Publication: eprint arXiv:gr-qc/0604017.

[8] R. M. Liang and K. S. Arun, "Parameter Estimation for Superimposed Chirp Signals," in *5th IEEE Int. Conf. on Acoustics, Speech, and Signal Processing*, San Francisco, USA, March 23-26 1992.

[9] X. Xia, "Discrete Chirp-Fourier Transform and Its Application to Chirp Rate Estimation," *IEEE Transactions on Signal Processing*, vol. 48, pp. 3122–3133, 2000.

[10] A. Brodzik, "On the Fourier Transform of Finite Chirps," *IEEE Signal Processing Letters*, vol. 13, no. 9, pp. 541–544, September 2006.

[11] D. Peacock and B. Santhanam, "Multicomponent Subspace Chirp Parameter Estimation Using Discrete Fractional Fourier Analysis," in *Proceedings of the IASTED International Conference Signal and Image Processing*, Dallas, USA, Dec. 14-16 2011.

[12] I. Daubechies, Y. Wang, and H. Wu, "ConceFT: Concentration of Frequency and Time via a multitapered synchrosqueezed transform," 2015, Publication: eprint arXiv:1507.05366 [math.ST].

[13] J. Xiao and P. Flandrin, "Multitaper Time-Frequency Reassignment for Nonstationary Spectrum Estimation and Chirp Enhancement," *IEEE Transactions on Signal Processing*, vol. 55, no. 6, pp. 2851–2860, June 2007.

[14] J. Guo, H. Zou, X. Yang, and G. Liu, "Parameter Estimation of Multicomponent Chirp Signals via Sparse Representation," *IEEE Transactions on Aerospace and Electronic Systems*, vol. 47, no. 3, pp. 2261–2268, July 2011.

[15] B. Wang and J. Huang, "Instantaneous Frequency Estimation of Multi-Component Chirp Signals in Noisy Enviroments," *Journal of Marine Science and Applications*, vol. 6, no. 4, pp. 13–17, Dec 2007.

[16] F. Auger and P. Flandrin, "Improving the Readability of Time-Frequency and Time-Scale Representations by the Reassignment Method," *IEEE Transactions on Signal Processing*, vol. 43, pp. 1068–1089, 1995.

[17] J. Swärd, J. Brynolfsson, A. Jakobsson, and M. Hansson-Sandsten, "Sparse Semi-Parametric Chirp Estimation," in *Asilomar Conference on Signals, Systems and Computers*, Asilomar, USA, 2-5 Nov 2014.

[18] L. Applebaum, S. Howard, S. Searle, and R. Calderbank, "Chirp sensing codes: Deterministic compressed sensing measurements for fast recovery," *Applied and Computational Harmonic Analysis*, vol. 26, no. 2, pp. 283–290, March 2009.

[19] P. Stoica and R. Moses, *Spectral Analysis of Signals*, Prentice Hall, Upper Saddle River, N.J., 2005.

[20] I. Orović, S. Stanković, and A. Draganić, "Time-Frequency Analysis and Singular Value Decomposition Applied to the Highly Multicomponent Musical Signals," *Acta Acustica united with Acustica*, vol. 100, no. 1, pp. 93–101, 2014.

[21] M. Christensen and A. Jakobsson, *Multi-Pitch Estimation*, Morgan & Claypool, 2009.

[22] S. I. Adalbjörnsson, A. Jakobsson, and M. G. Christensen, "Multi-Pitch Estimation Exploiting Block Sparsity," *Elsevier Signal Processing*, vol. 109, pp. 236–247, April 2015.

[23] M. G. Christensen and J. R. Jensen, "Pitch Estimation for Non-Stationary Speech," in *48th Annual Asilomar Conference on Signals, Systems, and Computers*, Pacific Grove, USA, Nov. 2-5 2014.

[24] Y. Doweck, A. Amar, and I. Cohen, "Joint Model Order Selection and Parameter Estimation of Chirps with Harmonic Components," *IEEE Transactions on Signal Processing*, vol. PP, pp. 1, 2015.

[25] S. Boyd, N. Parikh, E. Chu, B. Peleato, and J. Eckstein, "Distributed Optimization and Statistical Learning via the Alternating Direction Method of Multipliers," *Found. Trends Mach. Learn.*, vol. 3, no. 1, pp. 1–122, Jan. 2011.

[26] P. Stoica and P. Babu, "Sparse Estimation of Spectral Lines: Grid Selection Problems and Their Solutions," *IEEE Trans. Signal Process.*, vol. 60, no. 2, pp. 962–967, Feb. 2012.

[27] Y. Chi, L. L. Scharf, A. Pezeshki, and A. R. Calderbank, "Sensitivity to Basis Mismatch in Compressed Sensing," *IEEE Trans. Signal Process.*, vol. 59, no. 5, pp. 2182 –2195, May 2011.

[28] J. F. Sturm, "Using SeDuMi 1.02, a Matlab toolbox for optimization over symmetric cones," *Optimization Methods and Software*, vol. 11-12, pp. 625–653, August 1999.

[29] R. H. Tutuncu, K. C. Toh, and M. J. Todd, "Solving semidefinite-quadratic-linear programs using SDPT3," *Mathematical Programming Ser. B*, vol. 95, pp. 189–217, 2003.

[30] P. G. Bühlmann and S. van de Geer, *Statistics for High-Dimensional Data*, Springer Series in Statistics. Springer, 2011.

[31] E. J. Candès, M. B. Wakin, and S. Boyd, "Enhancing Sparsity by Reweighted l_1 Minimization," *Journal of Fourier Analysis and Applications*, vol. 14, no. 5, pp. 877–905, Dec. 2008.

[32] R. Chartrand and B. Wohlberg, "A Nonconvex ADMM Algorithm for Group Sparsity with Sparse Groups," in *38th IEEE Int. Conf. on Acoustics, Speech, and Signal Processing*, Vancouver, Canada, May 26-31 2013.

[33] M. A. T. Figueiredo and J. M. Bioucas-Dias, "Algorithms for imaging inverse problems under sparsity regularization," in *Proc. 3rd Int. Workshop on Cognitive Information Processing*, May 2012, pp. 1–6.

[34] J. Eckstein and D.P. Bertsekas, "On the Douglas-Rachford splitting method and the proximal point algorithm for maximal monotone operators," *Mathematical Programming*, vol. 55, pp. 293–318, April 1992.

[35] K. B. Petersen and M. S. Pedersen, "The Matrix Cookbook," http://matrixcookbook.com/.

[36] E. J. Candes and T. Tao, "Decoding by Linear Programming," *IEEE Transactions on Information Theory*, vol. 51, no. 12, pp. 4203–4215, Dec 2005.

[37] R. G. Baraniuk and D. L. Jones, "A Signal Dependent Time Frequency Representation: Optimal Kernel Design," *IEEE Transactions on Signal Processing*, vol. 41, pp. 1589–1602, April 1993.

Johan Swärd (S'12) received his M.Sc. from Lund University in Industrial Engineering and Management in 2012, Sweden, and is currently working towards a Ph.D. in Mathematical Statistics at Lund University. He has been a visiting researcher at the Department of Systems Innovations at Osaka University, Japan. His research interests include time-frequency analysis and applications of sparse and convex modeling in statistical signal processing and spectral analysis.

Johan Brynolfsson (S'12) received his M.Sc. in Mathematical Engineering from the University of Lund, Sweden, in 2012. He is currently working part time towards his Ph.D. in Mathematical Statistics, also at Lund University, where his main interest lies in time-frequency analysis. He is also working as a research engineer at Spectronic Medical, Sweden, where his main focus lies with neural network solutions in medical imaging.

Andreas Jakobsson (S'95-M'00-SM'06) received his M.Sc. from Lund Institute of Technology and his Ph.D. in Signal Processing from Uppsala University in 1993 and 2000, respectively. Since, he has held positions with Global IP Sound AB, the Swedish Royal Institute of Technology, King's College London, and Karlstad University, as well as held an Honorary Research Fellowship at Cardiff University. He has been a visiting researcher at King's College London, Brigham Young University, Stanford University, Katholieke Universiteit Leuven, and University of California, San Diego, as well as acted as an expert for the IAEA. He is currently Professor and Head of Mathematical Statistics at Lund University, Sweden. He has published his research findings in over 150 refereed journal and conference papers, and has filed five patents. He has also authored a book on time series analysis (Studentlitteratur, 2013 and 2015), and co-authored (together with M. G. Christensen) a book on multi-pitch estimation (Morgan & Claypool, 2009). He is a member of The Royal Swedish Physiographic Society, a Senior Member of IEEE, and an Associate Editor for Elsevier Signal Processing. He has previously also been a member of the IEEE Sensor Array and Multichannel (SAM) Signal Processing Technical Committee (2008-2013), an Associate Editor for the IEEE Transactions on Signal Processing (2006-2010), the IEEE Signal Processing Letters (2007-2011), the Research Letters in Signal Processing (2007-2009), and the Journal of Electrical and Computer Engineering (2009-2014). His research interests include statistical and array signal processing, detection and estimation theory, and related application in remote sensing, telecommunication and biomedicine.

Maria Hansson-Sandsten (M'96) was born in Sweden 1966. She received the MSc degree in Electrical Engineering in 1989 and a PhD degree in Signal Processing in 1996, both from Lund University in Sweden. Currently she is Professor in Mathematical Statistics at the Centre for Mathematical Sciences at Lund University. Her research interests include time-frequency analysis, multitaper spectrum analysis and feature extraction for detection, estimation and classification of biological and biomedical signals.